Entanglement of a Photon and an Optical Lattice Spin Wave

Y. O. Dudin,[1] S. D. Jenkins,[1] R. Zhao,[1] D. N. Matsukevich,[2] A. Kuzmich,[1] and T. A. B. Kennedy[1]
[1]School of Physics, Georgia Institute of Technology, Atlanta, Georgia 30332-0430
[2]Department of Physics, University of Maryland, College Park, Maryland 20742
(Received 1 April 2009; published 10 July 2009)

We propose and implement a scheme to produce long-lived entanglement between a signal field and a magnetically insensitive collective excitation in an atomic cloud cooled in a one-dimensional optical lattice. After a programmable storage time, we convert the spin-wave excitation into an idler field, and demonstrate violation of Bell's inequality for storage times in excess of 3 ms.

DOI: 10.1103/PhysRevLett.103.020505 PACS numbers: 03.67.Bg, 03.65.Ud, 37.10.Jk, 42.50.Dv

Matter-light entanglement is of great interest as a means to generate and distribute entanglement between remote parties [1]. In recent years, atomic systems have been investigated with the view towards quantum information processing in a network with quantum memory [2]. Matter-light entanglement has been reported using (a) collective matter excitations [3,4], (b) single neutral atoms [5,6], and (c) single ions [7,8]. The lifetime of these different matter qubits varies from less than 30 μs for collective spin waves, to 150 μs for single-atom qubits, while trapped ion qubits have a lifetime of several seconds. Continuous-variable entanglement of room-temperature atomic samples has been observed for the duration of 0.5 ms; see Ref. [9]. As neutral alkali atoms have transitions in the telecom wavelength band, it is important to increase the qubit lifetime in these systems for long-distance fiber network implementations [10,11]. In earlier experiments in neutral atomic systems, states with nonzero magnetic moment were employed, and the qubit lifetime was limited by uncompensated ambient magnetic fields [3–6,12–15]. The basis of these experiments is a two-stage Raman scattering process in a cloud of laser-cooled Rb atoms, separated by a storage period for the spin-wave excitation generated in the write process; see Fig. 1. A weak off resonant write laser pulse induces signal photon emission and correlated spin-wave excitation of the medium. After a delay, the atomic excitation is retrieved by a read laser which induces reverse Raman scattering with emission of an idler photon.

In this Letter, we measure Bell inequality violation between signal and idler fields as a function of the delay, up to a value of 3.3 ms. This is achieved by storing orthogonal magnetically insensitive spin waves while confining the atomic sample in a one-dimensional optical lattice to suppress the additional dephasing effects of atomic motion. In previous work, an optical lattice was used to demonstrate long-lived quantum memory and to realize a high-quality deterministic single-photon source [16]. There, the clock transition between $m = 0$ hyperfine ground states was employed to reduce magnetic sensitivity. By contrast, in this work the clock coherence plays a minor role and instead two orthogonal spin waves associated with the $m = \pm 1 \leftrightarrow m' = \mp 1$ coherences are used to encode the long-lived atomic qubit. Moreover, the atoms are prepared in the $F = 1$ rather than $F = 2$ hyperfine ground level. Storage of coherent light for 240 ms in an atomic Mott insulator was recently demonstrated in Ref. [17].

Raman scattering of the write field from the ensemble creates a pair of excitations: a signal photon, and a correlated collective atomic excitation. The latter is comprised of the clock spin wave $\hat{s}_{0,0}(z)$ and the magnetic spin waves $\hat{s}^H_{m_b,m_a}(z) \equiv -i[\hat{s}_{m_b,m_a}(z) + \hat{s}_{-m_b,-m_a}(z)]/\sqrt{2}$, $\hat{s}^V_{m_b,m_a}(z) \equiv [\hat{s}_{m_b,m_a}(z) - \hat{s}_{-m_b,-m_a}(z)]/\sqrt{2}$, where $\hat{s}_{m_b,m_a}(z)$ is the local spin-wave operator associated with the hyperfine transition $|b, m_b\rangle \leftrightarrow |a, m_a\rangle$; see Fig. 1. To lowest order in the coupling parameter $\chi \ll 1$, which scales with the product of dipole moments on the Raman transition and is inversely proportional to the write laser detuning [18], the joint signal-excitation density operator is given by $(1 + \chi\hat{\Phi}^\dagger)\hat{\rho}_0(1 + \chi\hat{\Phi})$, where $\hat{\rho}_0$ describes the atomic ground

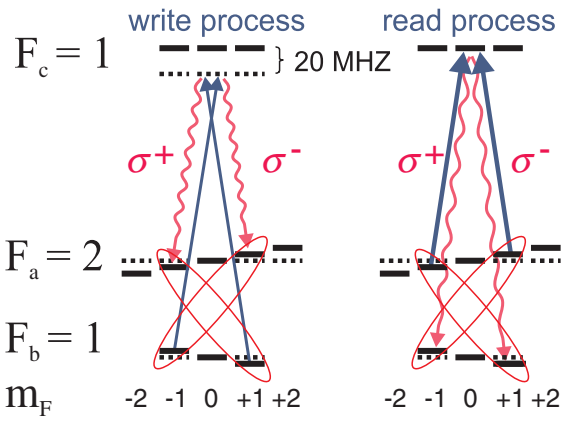

FIG. 1 (color online). The ^{87}Rb levels $|a\rangle$, $|b\rangle$, and $|c\rangle$, associated with the D_1 line at 795 nm used in the write or read protocol; see text. $\{|a\rangle; |b\rangle\}$ correspond to the $5S_{1/2}$, $F = \{2, 1\}$ levels, and $|c\rangle$ represents the $\{5P_{1/2}, F = 1\}$ level. The atoms are assumed to be prepared in states $|b, m\rangle$ with populations $p_{|m|}$. Orthogonally polarized write and read lasers are assumed to counterpropagate along the quantization, z, axis. The Zeeman shifts are determined by a bias magnetic field directed along the z axis.

state, and

$$\hat{\Phi} \equiv \cos\eta \hat{a}_V \hat{A}_H + \sin\eta \hat{a}_H \hat{A}_V, \quad (1)$$

where $\cos^2\eta = (3 + 5p_0)/(6 + 8p_0)$, $\hat{a}_H$ and $\hat{a}_V$ are horizontal and vertical signal annihilation operators. Here p_0 and $p_1 = p_{-1}$ are occupation probabilities of $|b, 0\rangle$ and $|b, \pm 1\rangle$, respectively, corresponding to an aligned state with zero orientation. The density operator describes an unpolarized atomic sample $p_0 = p_{\pm 1}$, as well as a more general atomic state determined by cycles of the write process prior to signal detection. The atomic excitations correlated with emission of horizontally or vertically polarized signal fields, are described by annihilation operators

$$\hat{A}_H = \frac{\sqrt{2p_0}(i\hat{S}_{0,0} - \sqrt{3}\hat{S}^H_{0,2}) - \sqrt{3p_1}(\hat{S}^H_{1,-1} + \hat{S}^H_{1,1})}{\sqrt{3 + 5p_0}}, \quad (2)$$

and

$$\hat{A}_V = -\frac{\sqrt{2p_0}\hat{S}^V_{0,2} - \sqrt{p_1}(\hat{S}^V_{1,-1} - \hat{S}^V_{1,1})}{\sqrt{1 + p_0}}, \quad (3)$$

respectively, where $\hat{S}^\lambda_{m_b,m_a} \equiv \int dz \sqrt{f(z)} \hat{s}^\lambda_{m_b,m_a}(z)$ and $\hat{S}_{0,0} \equiv \int dz \sqrt{f(z)} \hat{s}_{0,0}(z)$ are single-mode spin waves and $f(z) \equiv \bar{n}(z)/\int dz' \bar{n}(z')$ is the normalized spatial distribution function with $\bar{n}(z)$ the atomic density averaged over the transverse signal field mode [16]. We note that the emission of a horizontally polarized signal photon does not create a clock-type spin-wave excitation, but emission of both horizontally and vertically polarized photons results in a slowly varying spin excitation $S^{H/V}_{1,-1}$. The latter has a Larmor frequency proportional to the anomalous g factor δg, which is 500 smaller than the Larmor frequencies of the $S^{H/V}_{0,2}$ and $S^{H/V}_{1,1}$ spin waves. In a bias magnetic field $B_0\hat{z}$, the Larmor frequencies for Rb-87 are given by $\omega_{m_a,m_b} = (\mu_B B_0/\hbar)[g_a(m_a + m_b) - \delta g m_a] + O(B_0^2)$, where $g_a = 0.4998$ and $g_b = -0.5018$ are Landé factors and $\delta g \equiv g_a + g_b = -0.002$. Since δg is so small the $O(B_0^2)$ contribution to the frequency $\omega_{1,-1}$ is not negligible [19].

The spin-wave excitations are stored for a time T_s following the detection of the signal field. During this time the spin waves precess in the ambient magnetic field. As the field may vary spatially and temporally across the sample, the magnetic spin waves are dephased by the Zeeman effect. The corresponding dephasing rate is proportional to the spin-wave Larmor frequencies and therefore the $S_{0,0}$ and $S^{H/V}_{1,-1}$ spin waves are long-lived [16]. Under our experimental conditions the fast decoherence time $t_f \sim 100$ μs while the decoherence times for $S_{0,0}$ and $S^{H/V}_{1,-1}$ are expected to exceed the maximum storage time 3.3 ms employed here. Atomic motion is a more serious limitation for a freely expanding atomic cloud. As shown in our previous work [16], this may be offset by loading the atoms into a one-dimensional optical lattice which preserves the spin-wave grating.

Following the storage period, a read field of Rabi frequency Ω induces Raman conversion of the stored excitations into horizontally and vertically polarized idler fields, $\hat{\varphi}_H$ and $\hat{\varphi}_V$. For the atom-field configuration of Fig. 1, the readout can be understood in terms of the dark-state polariton mechanism [20]. The local annihilation operators for the horizontally and vertically polarized polaritons are given by, with $\kappa\sqrt{\bar{n}}$ the dipole coupling frequency,

$$\hat{\Psi}_H(z) = \frac{\Omega^*\hat{\varphi}_H + \kappa^*\sqrt{5\bar{n}/6}[\sqrt{3p_0/8}(\sqrt{3}\hat{s}^H_{0,2} - i\hat{s}_{0,0}) + \sqrt{p_1}(\hat{s}^H_{1,1} + \hat{s}^H_{1,-1})]}{\sqrt{|\Omega|^2 + 5\bar{n}|\kappa|^2(2 + p_0)/12}}, \quad (4)$$

$$\hat{\Psi}_V(z) = \frac{\Omega^*\hat{\varphi}_V + \kappa^*\sqrt{5\bar{n}/6}[\sqrt{2p_0}\hat{s}^V_{0,2} + \sqrt{p_1}(\hat{s}^V_{1,1} + \hat{s}^V_{1,-1})]}{\sqrt{|\Omega|^2 + 5\bar{n}|\kappa|^2(1 + p_0)/6}}. \quad (5)$$

The joint signal-idler detection rates are given by

$$C(\theta_s, \theta_i; T_s) \propto |\cos\eta[\hat{\Upsilon}_H(T_s), \hat{A}^\dagger_H]\sin\theta_s \cos\theta_i - \sin\eta[\hat{\Upsilon}_H(T_s), \hat{A}^\dagger_H]\cos\theta_s \sin\theta_i|^2, \quad (6)$$

where $\hat{\Upsilon}_H(T_s) = \int dz \sqrt{f(z)} \Psi_H(z, T_s)|_{\Omega=0}$, θ_s and θ_i are signal and idler polarization angle settings, respectively, with $\theta_{s,i} = 0$ corresponding to horizontally polarized fields. The commutators quantify the overlap of the written spin waves [Eqs. (2) and (3)] with the matter excitation available for readout [Eqs. (4) and (5)] and its dependence on the alignment of the initial atomic state. Measurements of these joint detection rates, as a function of T_s, enable us to determine the Bell parameter S and thus to study violation of Bell's inequality $|S| \leq 2$. The commutators in Eq. (6) involve spatial integration of phase factors in which a spatially varying Larmor frequency multiplies T_s. This is the origin of the spin-wave dephasing, washing out fast spin waves in a time $T_s \simeq 100$ μs, leaving only the slow spin-wave contributions at longer times.

The main elements of our experiment are shown in Fig. 2. A sample of 10^9 Rb-87 atoms is collected and cooled in a magneto-optical trap for a period of 0.5 s. The trap laser is then detuned 90 MHz below atomic resonance, the quadrupole magnetic field is turned off and the repump laser intensity is lowered for 20 ms, in

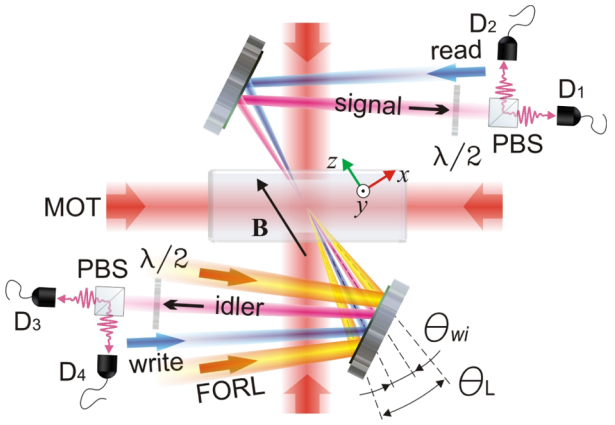

FIG. 2 (color online). Schematic of optical lattice spin-wave qubit implementation. An atomic sample of about 10^7 ^{87}Rb atoms is loaded from a magneto-optical trap (MOT) in a 1D far off resonant optical lattice (FORL) of the 25 μm period, formed by interfering two 7 W, 1.06 μm beams with an angular separation $\theta_L = 2.5°$. A bias magnetic field B points in the z direction. The beam waists, $1/e^2$, are 150 μm and 170 μm, respectively, giving a maximum trap depth of 100 μK. The write and read fields share a single spatial mode of waist 370 μm, while the signal and idler mode waist is 110 μm. The write/read and signal/idler modes intersect at the position of the atomic sample at an angle $\theta_{wi} = 0.9°$. PBS is a polarizing beam splitter, and $\lambda/2$ labels a half-wave plate, D_1 through D_4 are single-photon detectors.

order to optimize sub-Doppler cooling and loading of the optical lattice. As a result, the lattice contains about 10^7 atoms in the $5S_{1/2}$, $F = 1$ hyperfine level. The lattice parameters, see caption of Fig. 2, result in the oscillation frequencies 3×10^3, 200, and 8 Hz. The transverse temperature of the cloud was measured to be 20 μK.

After loading, we apply a 0.66 G bias magnetic field in the z direction and initiate a write or signal measurement sequence of maximum duration 36 ms. The sequence begins with a 50 ns long vertically polarized incident write pulse of power 1 μW. The pulse is detuned by -20 MHz from the $|b\rangle \rightarrow |c\rangle$ transition. The Raman scattered signal field, on the $|c\rangle \rightarrow |a\rangle$ transition, is collected and passed through a half-wave plate, and a polarizing beam splitter followed by single-photon detectors D_1 and D_2. In the absence of a photoelectric detection event registered by either D_1 or D_2, the write pulse is followed by an orthogonally polarized clean pulse, duration 200 ns, power 270 μW, which transfers atomic population back from $|a\rangle$ to $|b\rangle$, and the sequence is repeated at a frequency of 0.66 MHz. A detection event at D_1 or D_2 (with probability 10^{-4}) heralds the excitation of an atomic spin wave with the desired wave vector and the write or signal measurement sequence is stopped.

The collective atomic excitation is stored for a time $2\pi n/\omega_{1,-1} = 0.54n$ ms for $B_0 = 0.66$ G, where n is an integer. Then a horizontally polarized read laser pulse (identical to the clean pulse), and counterpropagating

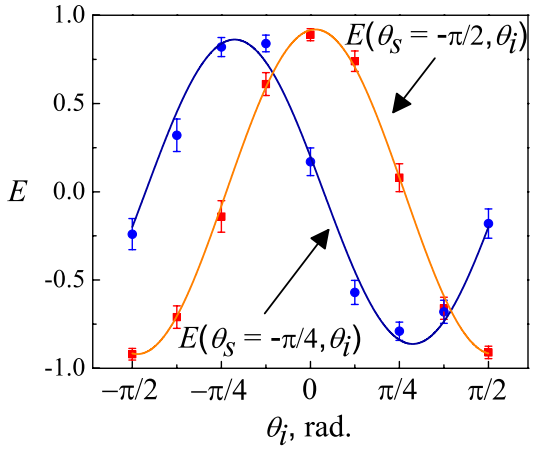

FIG. 3 (color online). Measured correlation function $E(\theta_s, \theta_i)$ after the first Larmor period of $2\pi/\omega_{1,-1} = 0.54$ ms. The curves are sinusoidal fits to the data.

with the write pulse, induces Raman scattering, converting the stored spin-wave excitation into an idler field emitted on the $|c\rangle \rightarrow |b\rangle$ transition. The write, read, and detected signal and idler field wave vectors satisfy the phase-matching condition $\mathbf{k}_w + \mathbf{k}_r = \mathbf{k}_s + \mathbf{k}_i$, ensuring high-efficiency readout of the spin-wave excitation. The idler field is passed through a half-wave plate, followed by a polarizing beam splitter, onto a pair of single-photon detectors D_3 and D_4. To account for unequal propagation and detection efficiencies, the signal and idler polarizations are rotated by $\pi/2$ every 20 min. The idler photodetection probability varied between 0.5% and 0.25% for the data presented in Fig. 4.

The resulting joint signal-idler detection rates $C_{ij}(\theta_s, \theta_i)$, $i = 1, 2$, $j = 3, 4$ exhibit sinusoidal variations as a function of the orientations of the wave plates, in

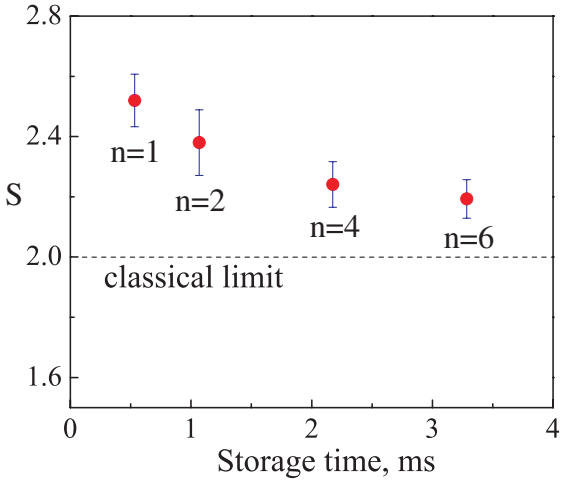

FIG. 4 (color online). Measured values of the Bell parameter S as a function of storage time, for an integer number $n = 1, 2, 4, 6$ of Larmor periods of 0.54 ms.

TABLE I. Measured correlation function $E(\theta_s, \theta_i)$ and S for 3.3 ms storage time based on 2702 events.

θ_s	θ_i	$E(\theta_s, \theta_i)$
$-\pi/2$	$\pi/8$	0.474 ± 0.033
$-\pi/2$	$-\pi/8$	0.630 ± 0.030
$-\pi/4$	$\pi/8$	0.593 ± 0.031
$-\pi/4$	$-\pi/8$	-0.496 ± 0.034
		$S_{\text{exp}} = 2.19 \pm 0.06$

agreement with Eq. (6). We check for Bell inequality violation $|S| \leq 2$ by measuring polarization correlations between signal and idler fields at certain canonical angles, where $S = E(-\pi/2, -\pi/8) + E(-\pi/2, \pi/8) + E(-\pi/4, -\pi/8) - E(-\pi/4, \pi/8)$, here the correlation function $E(\theta_s, \theta_i)$ is given by [21,22]

$$\frac{C_{13}(\theta_s, \theta_i) + C_{24}(\theta_s, \theta_i) - C_{14}(\theta_s, \theta_i) - C_{23}(\theta_s, \theta_i)}{C_{13}(\theta_s, \theta_i) + C_{24}(\theta_s, \theta_i) + C_{14}(\theta_s, \theta_i) + C_{23}(\theta_s, \theta_i)}.$$

The measured sinusoidal variation of $E(\theta_s, \theta_i)$ as a function of θ_i for fixed θ_s is shown in Fig. 3. In Fig. 4 we show the measured Bell parameter S after $n = 1, 2, 4$, and 6 Larmor periods: for $n = 6$ (a 3.3 ms storage period) the data are presented in Table I. The acquisition time varied from 5 h ($n = 1$) to 32 h ($n = 6$) for the data points in Fig. 4. As one might expect, $|S|$ decreases, but exceeds 2 by more than 3 standard deviations. The rate of decay is consistent with motional dephasing due to differential light shifts, as previously observed [16], while the expected magnetic decoherence rates of the slow coherences are at least an order of magnitude smaller.

From the theoretical analysis presented earlier, Eq. (6), we can calculate the Bell parameter as a function of p_0. For the canonical angles chosen in the experimental measurements, we find that $|S|$ is a monotonically decreasing function $\sqrt{2} \leq |S| \leq 2\sqrt{2}$. Rather than give a full analytic expression, we plot $|S|$ in Fig. 5 and note that for $p_0 \ll 1$, $|S| = 2\sqrt{2} - \frac{25}{16\sqrt{2}}(p_0^2 + \frac{1}{2}p_0^3) + O(p_0^4)$. From Fig. 5, the short time data of Fig. 4 is consistent with values of $p_0 \leq 0.6$, including $p_0 = 1/3$ for an unpolarized sample. Numerical calculations of the protocol suggest that p_0 falls from its initial value of $1/3$ to a steady state value of 0.15 within the first few milliseconds of the 36 ms write protocol. The population's dynamics are under experimental investigation and will be reported elsewhere [23].

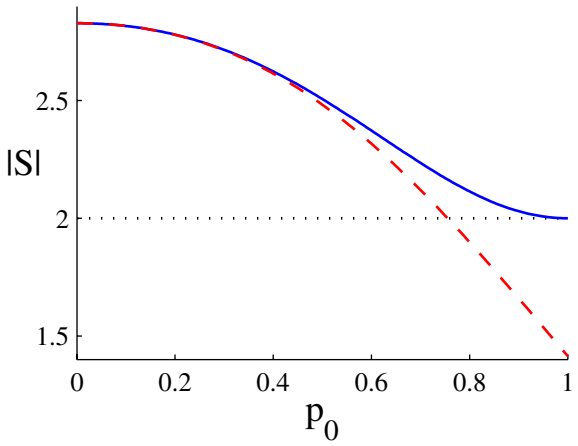

FIG. 5 (color online). Theoretical values of Bell's parameter as a function of p_0 for the canonical angles used in the experiment (dashed curve) and for optimized angles (solid curve).

In summary, we have observed violation of Bell's inequality for idler and signal fields with the idler delayed by up to 3.3 ms. The idler storage time could be increased substantially by employing a blue-detuned optical lattice and further reducing the atomic temperature.

This work was supported by the National Science Foundation, A. P. Sloan Foundation, and the Air Force Office of Scientific Research.

[1] H.-J. Briegel *et al.*, Phys. Rev. Lett. **81**, 5932 (1998).
[2] L.-M. Duan, M. D. Lukin, J. I. Cirac, and P. Zoller, Nature (London) **414**, 413 (2001).
[3] D. N. Matsukevich and A. Kuzmich, Science **306**, 663 (2004).
[4] D. N. Matsukevich *et al.*, Phys. Rev. Lett. **95**, 040405 (2005).
[5] J. Volz *et al.*, Phys. Rev. Lett. **96**, 030404 (2006).
[6] W. Rosenfeld *et al.*, Phys. Rev. Lett. **101**, 260403 (2008).
[7] B. B. Blinov, D. L. Moehring, L.-M. Duan, and C. Monroe, Nature (London) **428**, 153 (2004).
[8] D. L. Moehring *et al.*, Phys. Rev. Lett. **93**, 090410 (2004).
[9] B. Julsgaard, A. Kozhekin, and E. S. Polzik, Nature (London) **413**, 400 (2001).
[10] T. Chanelière *et al.*, Phys. Rev. Lett. **96**, 093604 (2006).
[11] S. D. Jenkins *et al.*, J. Opt. Soc. Am. B **24**, 316 (2007).
[12] D. N. Matsukevich *et al.*, Phys. Rev. Lett. **97**, 013601 (2006).
[13] J. Simon, H. Tanji, S. Ghosh, and V. Vuletic, Nature Phys. **3**, 765 (2007).
[14] Y. A. Chen *et al.*, Nature Phys. **4**, 103 (2008).
[15] K. S. Choi, H. Deng, J. Laurat, and H. J. Kimble, Nature (London) **452**, 67 (2008).
[16] R. Zhao *et al.*, Nature Phys. **5**, 100 (2009).
[17] U. Schnorrberger *et al.*, arXiv:0903.0135 [Phys. Rev. Lett. (to be published)].
[18] T. Chanelière *et al.*, Phys. Rev. Lett. **98**, 113602 (2007).
[19] D. M. Harber, H. J. Lewandowski, J. M. McGuirk, and E. A. Cornell, Phys. Rev. A **66**, 053616 (2002).
[20] M. Fleischhauer and M. D. Lukin, Phys. Rev. Lett. **84**, 5094 (2000).
[21] J. S. Bell, Physics (Long Island City, N.Y.) **1**, 195 (1964); J. S. Bell, Rev. Mod. Phys. **38**, 447 (1966).
[22] J. F. Clauser, M. A. Horne, A. Shimony, and R. A. Holt, Phys. Rev. Lett. **23**, 880 (1969).
[23] S. D. Jenkins *et al.* (to be published).